Quantum Mechanical Studies of Pressure Effects in Crystalline Ammonium Dinitramide

Dan C. Sorescu*,† and Donald L. Thompson

Department of Chemistry, Oklahoma State University, Stillwater, Oklahoma 74078

Received: March 28, 2001; In Final Form: May 29, 2001

Plane-wave ab initio calculations based on density function theory and the pseudopotential method have been used to investigate the structural properties of crystalline ammonium dinitramide (ADN) under hydrostatic compression in the pressure range 0−300 GPa. Optimization of the crystal structure has been done with full relaxation of atomic positions and lattice parameters without any symmetry constraints. The calculations were performed using periodic boundary conditions in all three directions. Changes in the electronic bands, charge distributions, and geometric parameters of the crystal have been computed as functions of pressure. We find that the ADN crystal maintains its monoclinic structure with $P2_1/c$ symmetry for pressures up to 10 GPa, where there is a transition to a $P\bar{1}$ triclinic symmetry. The crystalline phase transition involves reorientation of the ammonium ions relative to the dinitramide ions as well as additional rotations of the NO_2 groups relative to the N−N−N plane of dinitramide ions.

I. Introduction

There is considerable interest in finding environmentally benign replacements for the energetic oxidizer ammonium perchlorate (AP), which is currently used in rocket propellants, since it produces HCl as a combustion product. Dinitramide salts are viewed as promising candidates.[1] Consequently, understanding the fundamental electronic and structural properties of these compounds is important for the development of new propellants.

The dinitramide anion (DN^-), $N(NO_2)_2^-$, can be prepared in combination with various inorganic and organic counterions, including ammonium, lithium, potassium, and cesium,[2] biguanidinium,[3] and dinitro azetidinium.[4] Some of the critical properties of these compounds, e.g., shock and heat sensitivities, are influenced by the crystal structure and the nature of intermolecular forces. The structure of the DN^- ion has been the subject of several theoretical studies.[5−7] In the gas phase the equilibrium structure of DN^- has C_2 symmetry. However, in the condensed phases the anion generally does not have internal symmetry due to the steric and electronic properties of its environment, except in the cases of the lithium salt, in which DN^- has C_2 symmetry, and the dinitroazetidinium salt, in which DN^- has mirror symmetry.[2] These studies indicate that the conformation of DN^- is highly dependent on its environment.

Ammonium dinitramide (ADN), $NH_4N(NO_2)_2$, has been identified as a promising energetic material and is, to some extent, serving as the prototypical dinitramide salt. It is a powerful oxidizer without the environmental problems of AP. Consequently, several experimental studies of it have been reported in recent years.[8−15]

The crystal structure of ADN at ambient pressure has been resolved by X-ray diffraction measurements.[2] The unit cell is monoclinic with $P2_1/c$ crystal symmetry and with four molecules ($[NH_4]^+[N_3O_4]^-$) per unit cell (see Figure 1). There is strong hydrogen bonding involving all four ammonium hydrogen atoms with the oxygen atoms of the surrounding DN^- ions. There have been a number of experimental studies of the decomposition of ADN. Rossi et al.[8] have carried out mechanistic studies of its thermal decomposition by using mass spectroscopy. Brill et al.[9] used T-jump/FTIR to investigate the thermal decomposition mechanism. These studies were carried out under conditions (either low pressures or high temperatures) that favor gas-phase reactions. The results suggest two main pathways: $NH_4N(NO_2)_2 \rightarrow NH_3 + HNO_3 + N_2O$ and $NH_4N(NO_2)_2 \rightarrow NH_3 + HN(NO_2)_2$. These reactions are analogous to those postulated for ammonium nitrate (AN) and AP, that is, dissociative vaporization giving ammonia and the corresponding acid. The condensed phase thermal decomposition has also been studied. Russell et al.[10] obtained results indicating that there is a low-temperature (below 130 °C) reaction pathway in which ADN is converted to AN and N_2O and another mechanism at high temperatures where the decomposition begins with N−N bond fission to form NO_2. Vyazovkin and Wight[11] have recently reported the results of experiments of the thermal decomposition under conditions relevant to propellant combustion. They postulate a mechanism with two steps: $NH_4N(NO_2)_2 \rightarrow NH_4NO_3 + N_2O$ and $NH_4N(NO_2)_2 \rightarrow NH_4NNO_2 + NO_2$. Russell et al.[15] determined the pressure−temperature−reaction phase diagram for ADN between −125 and 120 °C up to 10 GPa. They found a reversible $\alpha \rightarrow \beta$ phase transition at 2 GPa. The α-phase melts at 95 °C; melting involves thermal decomposition above
136 °C.

These investigations of the thermal decomposition provide incentive for the initiation of studies to model the behavior of this potentially useful oxidizer. Our initial focus is on the physical properties of ADN. In a previous study[16] we have extensively investigated theoretically the structural properties of ADN crystal structure at ambient pressure. This has been done based on first-principles calculations using density functional theory (DFT) and the pseudopotential method with periodic boundary conditions in all three directions. The equilibrium structure of the crystal was obtained by full relaxation of the unit cell parameters allowed by the $P2_1/c$ crystal symmetry as well as of the ionic positions inside the unit cell.

* Corresponding author.
† Current mailing address: Department of Chemistry, University of Pittsburgh, Pittsburgh, PA 15260.

10.1021/jp011175d CCC: $20.00
Published on Web 07/13/2001

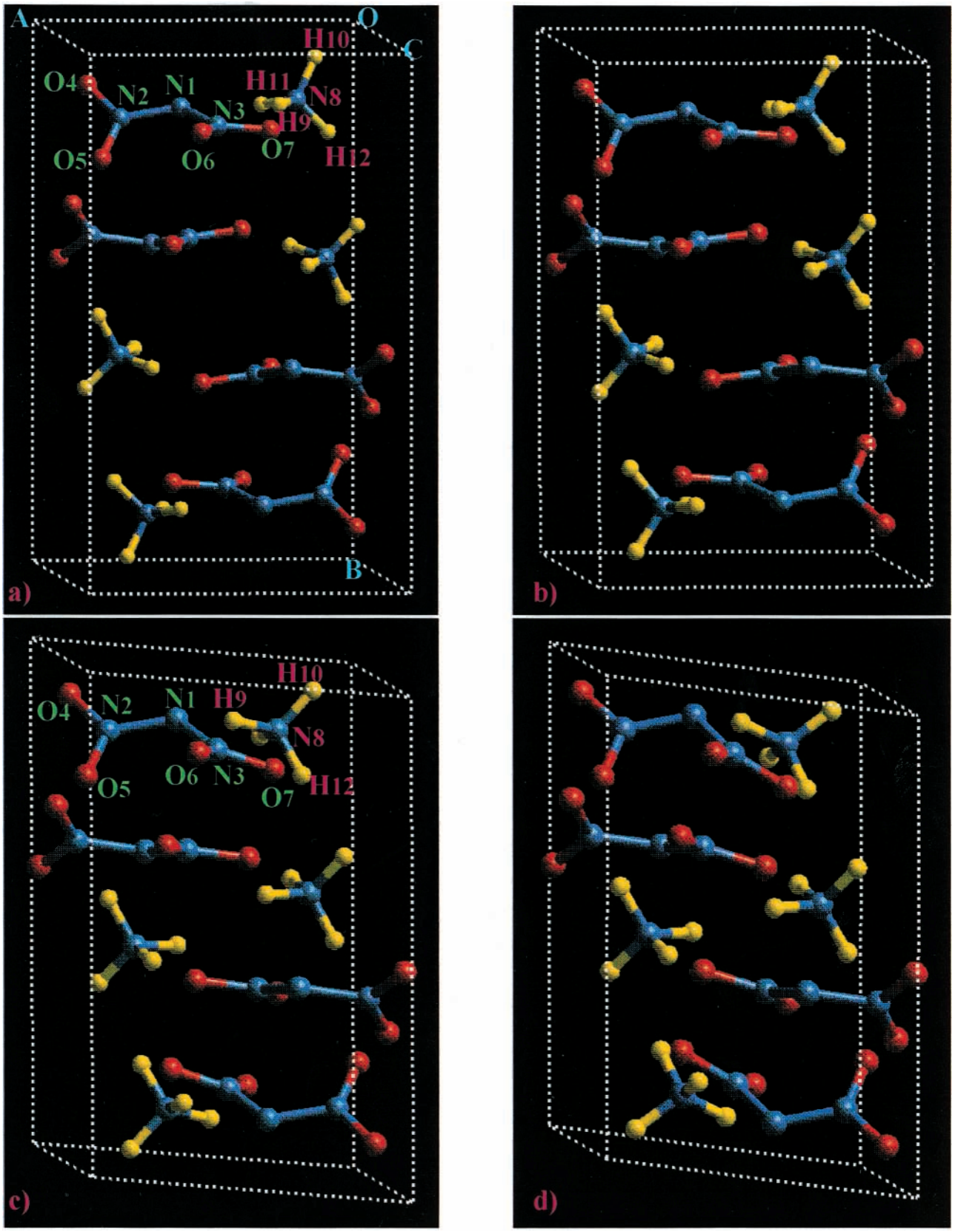

Figure 1. Pictorial views of the ADN crystal structures predicted in the present study at pressures: (a) 0 GPa; (b) 10 GPa; (c) 40 GPa; (d) 150 GPa.

Our results, in agreement with experiment,[2] indicate that the DN^- ions do not have internal symmetry. The two halves of the dinitramide ion are twisted with respect to each other while the NO_2 groups are rotated out of the N−N−N plane. We have also developed an intermolecular potential that describes the structure of the ADN crystal in the approximation of rigid ions. This potential was composed of pairwise Lennard-Jones, hydrogen-bonding terms, and Coulombic interactions. The main crystallographic features of ADN crystal and its crystal energy are accurately reproduced in crystal-packing calculations with

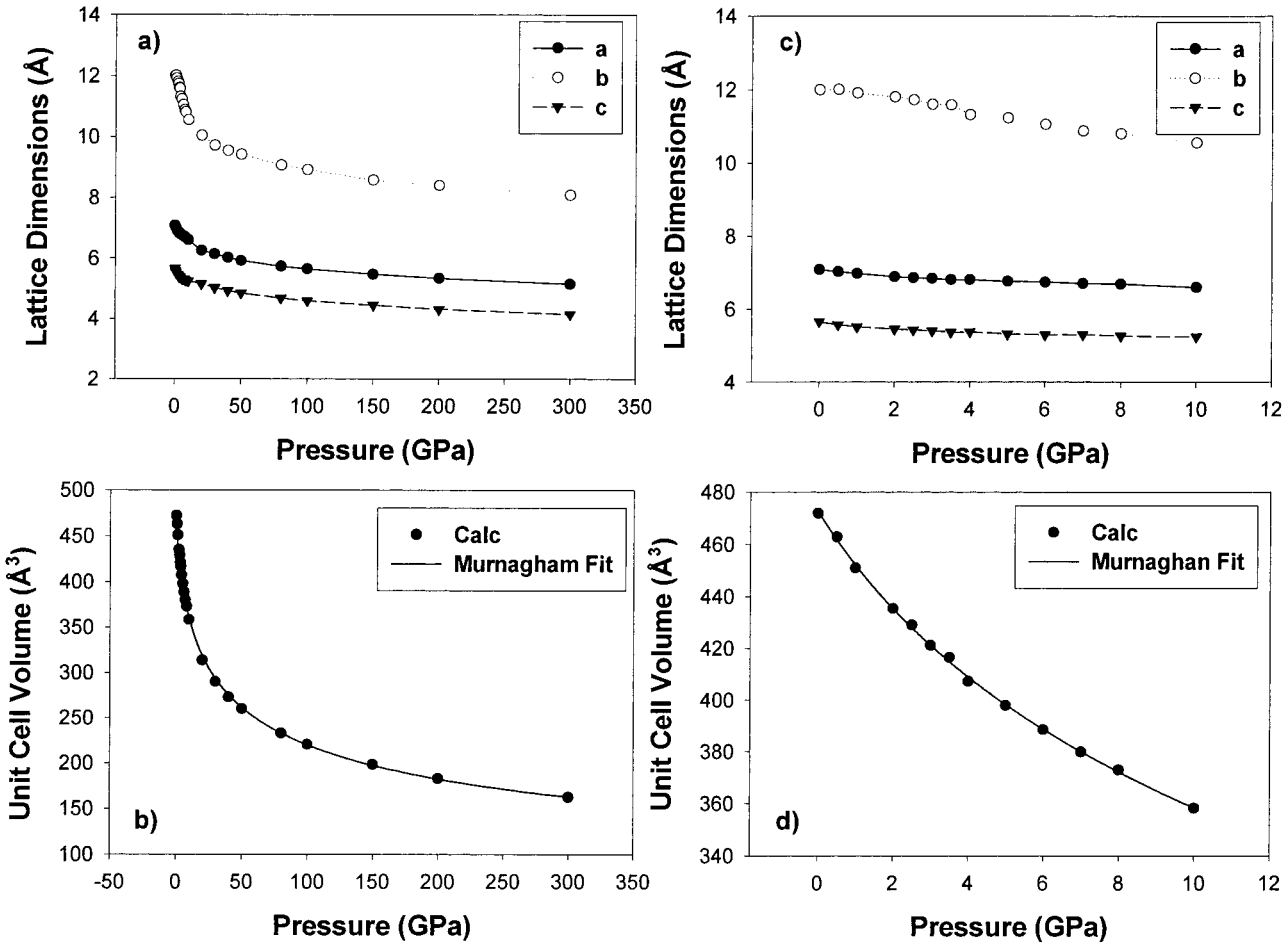

Figure 2. Variation of the (a) lattice dimensions and (b) unit cell volume of the ADN crystal structure as functions of the applied hydrostatic pressure. These quantities at low pressures (0−10 GPa) are detailed in (c) and (d).

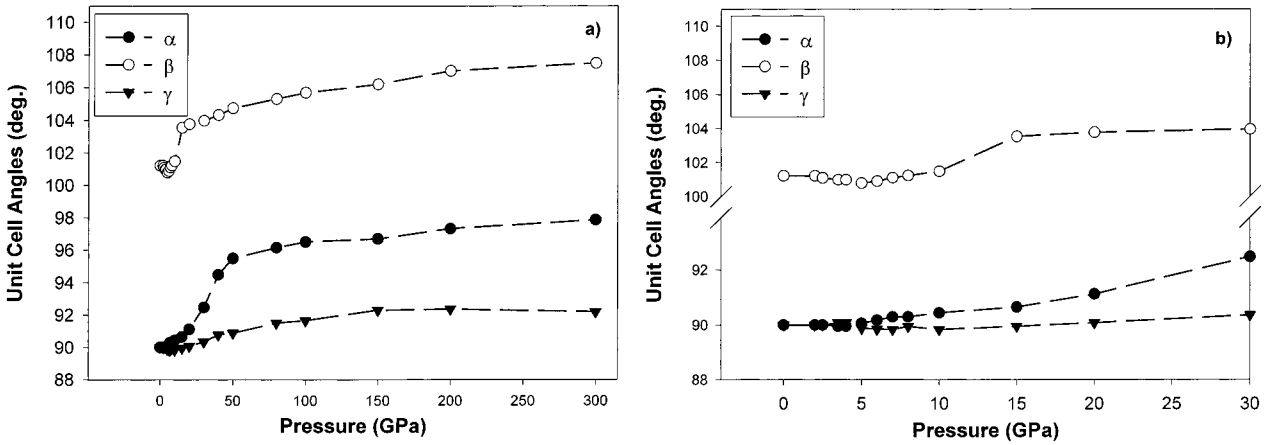

Figure 3. (a) Variation of the unit cell angles of the ADN crystal structure as functions of the applied hydrostatic pressure. The low-pressure regime (0−15 GPa) is detailed in frame (b).

this potential. Moreover, we have shown[16] based on molecular dynamics simulations that the main temperature effect on the lattice structure is an increase of the rotational disorder of the ammonium ions without any significant change in the translational order of these ions. The thermal expansion coefficients calculated with this model indicate anisotropic behavior with the largest expansion along the *b* crystallographic axis.

In the present study we extend our previous investigations of crystalline ADN by analyzing hydrostatic compression effects. Previous experimental studies[15] have shown the presence of two polymorphic states for crystalline ADN as function of pressure. The α-ADN phase corresponds to the low pressures regime and is stable up to 2.0 GPa. This phase melts between 92 °C and 95 °C depending on the amount of ammonium nitrate impurity present.[17] At about 2.0 GPa the α phase transforms to monoclinic *β*-ADN. This phase is stable above 2.0 GPa in the temperature range −75 to 140 °C. Above 140 °C between 1.0 and 10.0 GPa, ADN undergoes a molecular rearrangement with formation of ammonium nitrate and N_2O.

The main objective in the present work is to study the variations in the structural and electronic properties of ADN crystal as functions of hydrostatic compression of the crystal.

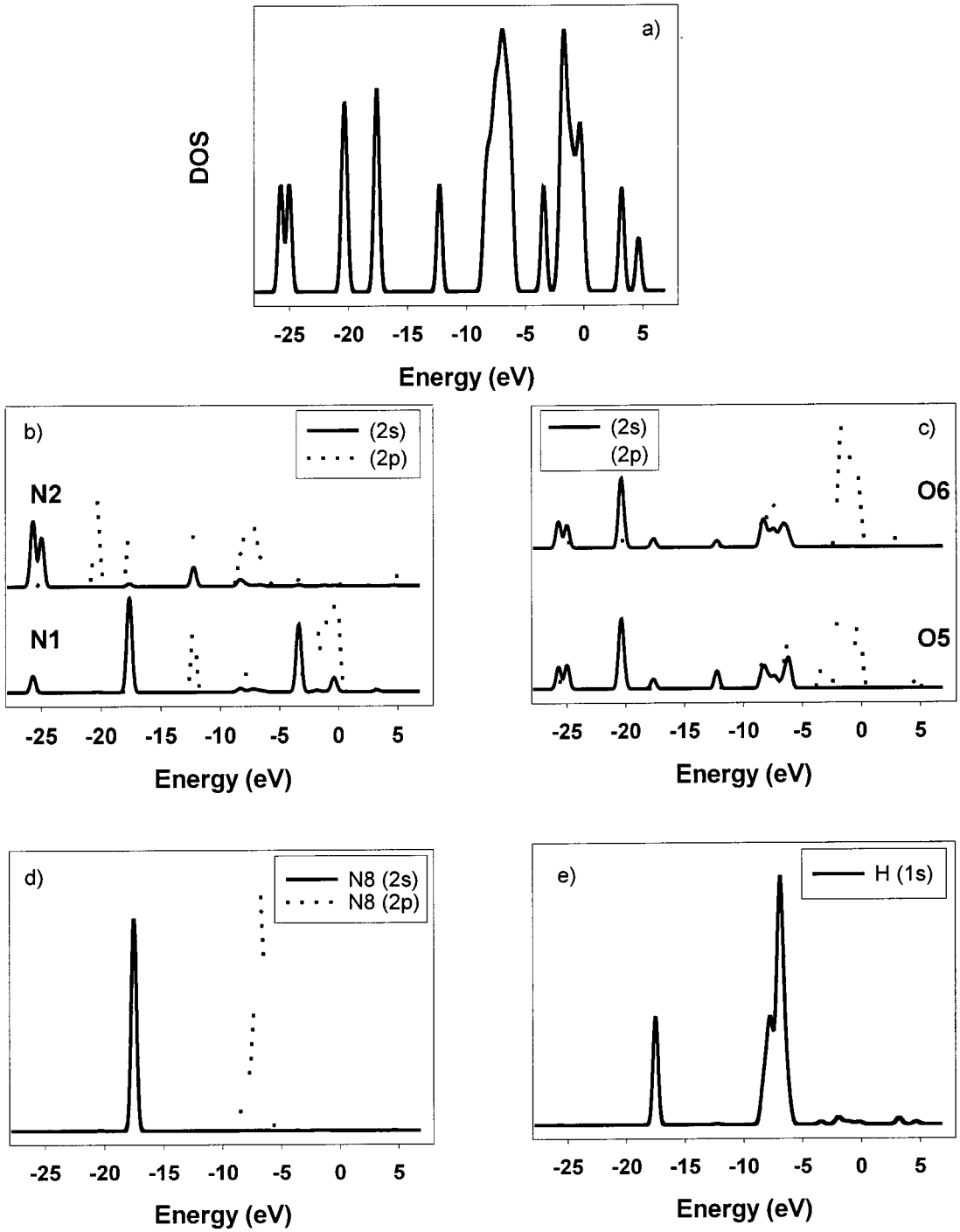

Figure 4. (a) Calculated total density of states (DOS) of ADN and (b−d) the projected density of states (PDOS) on selected atoms of DN^- and NH_4^+ at ambient pressure.

The methodology followed here is similar to that used in our previously study[16] and is based on first-principles calculations using density functional theory (DFT) and a pseudopotential method. The periodic nature of the crystal is considered in the present calculations by using boundary conditions in all three directions. The equilibrium structure of the crystal is obtained by full relaxation of the unit cell parameters allowed by the crystal symmetries as well as of the ionic positions inside the unit cell. Since our calculations do not include temperature effects the results correspond to very low temperatures below the range currently used in experimental investigations, i.e., −75 °C.[15]

The organization of the paper is as follows: In Section II we describe the computational methods. The results of total energy calculations for hydrostatic compression up to 300 GPa are given in Section III. Finally, we summarize the main conclusions in Section IV.

II. Computational Method

Total Energy Calculations. The calculations were performed using the commercial version of the software package CASTEP (Cambridge Serial Total Energy Package).[18] This program evaluates the total energy of periodically repeating geometries based on DFT and the pseudopotential approximation. In the latter, only the valence electrons are represented explicitly in the calculations, the valence−core interactions being described by nonlocal pseudopotentials. Periodic boundary conditions are

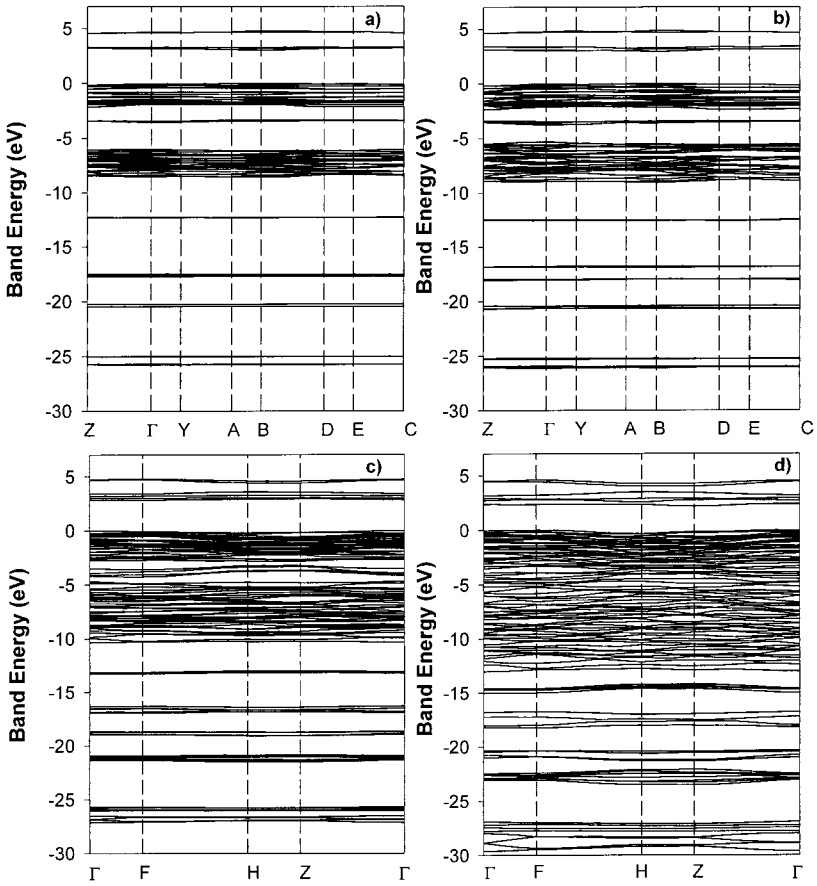

Figure 5. Calculated band structure for ADN at pressures: (a) 0 GPa; (b) 10 GPa; (c) 40 GPa; (d) 150 GPa. The energies of the highest occupied crystalline orbitals have been set to zero. The indicated k-points labels correspond to the following coordinates: Γ (0.0,0.0,0.0), Z(0.0,0.0,0.5), Y(0.0,0.5,0.0), A(−0.5,0.5,0), B(−0.5,0.0,0.0), D(−0.5,0.0,0.5), E(−0.5,0.5,0.5), C(0.0,0.5,0.5), F(0.0,0.5,0.0), H(0.0,0.5,0.5).

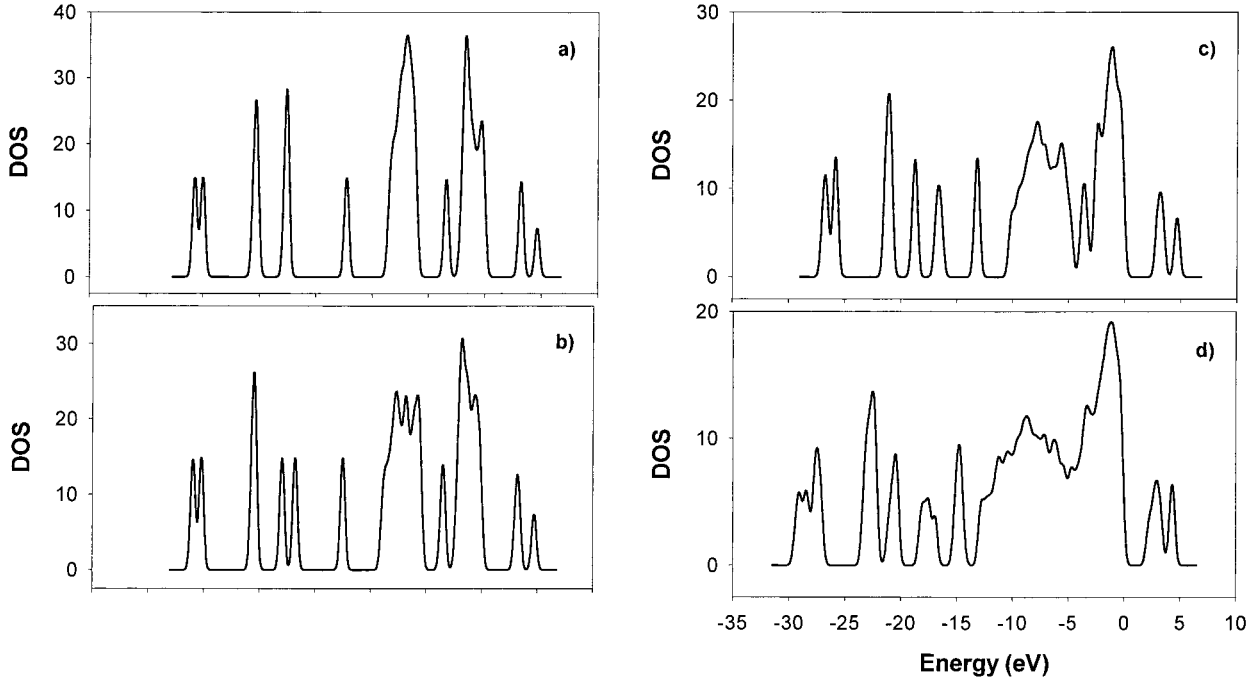

Figure 6. Calculated DOS for ADN at the pressures (a) 0 GPa; (b) 10 GPa; (c) 40 GPa; (d) 150 GPa.

used, with the occupied electronic orbitals expanded in a plane-wave basis. The expansion includes all plane waves with kinetic energies, $\hbar^2k^2/2m < E_{cut}$, where k is the wave vector, m the electronic mass, and E_{cut} is the chosen cutoff energy. The value of the cutoff energy is chosen to ensure convergence with respect to the basis set. A gradient-corrected form of the exchange correlation functional (GGA) was used in the manner suggested by White and Bird.[19] The Brillouin zone was sampled with the Monkhorst-Pack scheme.[20]

The pseudopotentials used in this study are norm-conserving of the form suggested by Kleinman and Bylander,[21] and optimized using the scheme of Lin et al.[22] The self-consistent

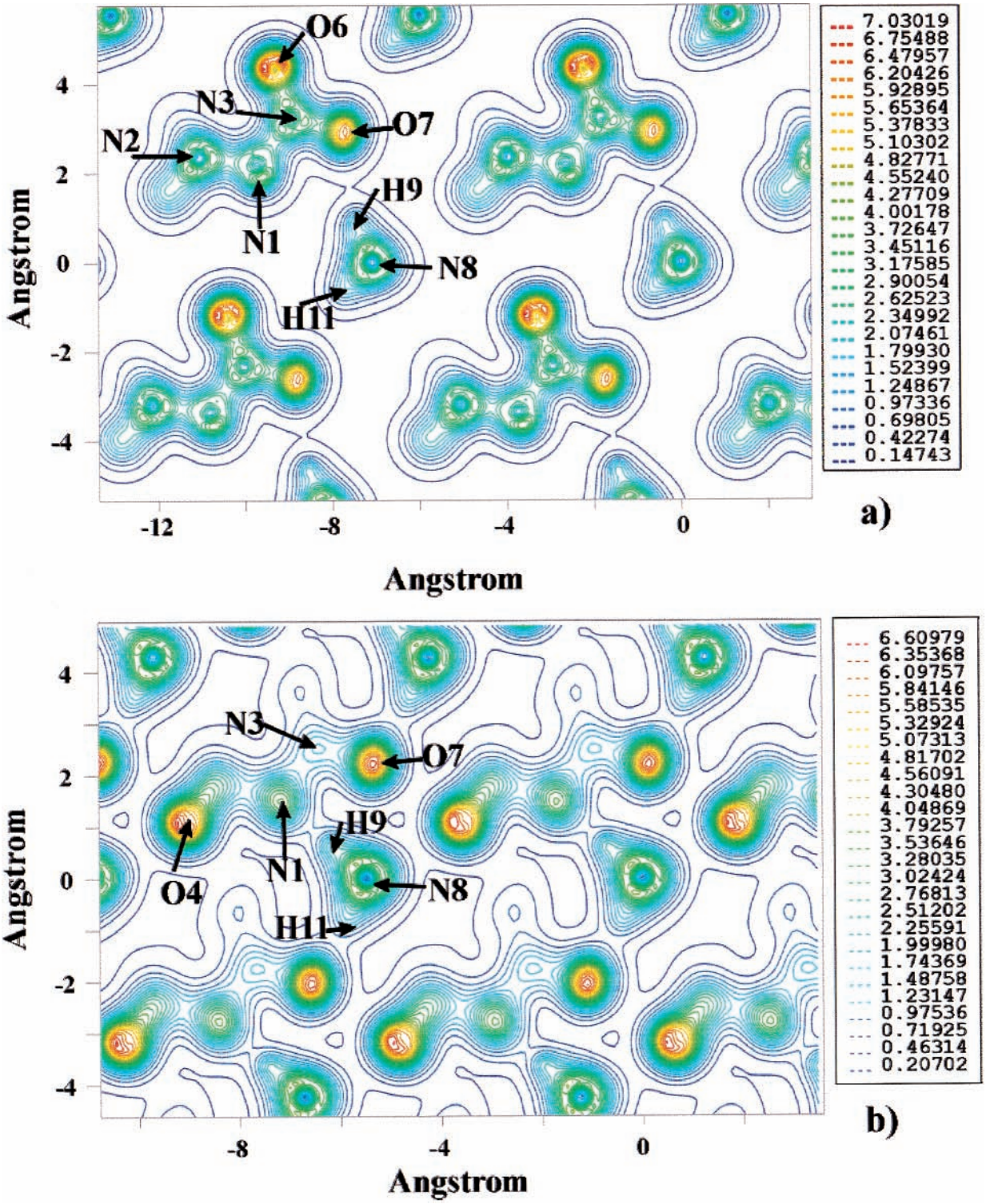

Figure 7. Contour plots of the valence electron density (units of electrons/Å^3) in the ADN crystal at the pressures: (a) 0 GPa and (b) 150 GPa. The contours are taken parallel to the aOc plane passing through the N_8 atoms of NH_4^+ ions.

ground state of the system was determined using a band-by-band conjugate gradient technique to minimize the total energy of the system with respect to the plane-wave coefficients. The optimization of different atomic configurations reported in this study was done using the Broyden-Fletcher-Goldfarb-Shanno (BFGS) minimization technique, with the following thresholds for the converged structure: energy change per atom less than 2.0×10^{-5} eV, residual force less than 0.05 eV/Å, the displacement of atoms during the geometry optimization less than 0.001 Å, and the residual bulk stress less than 0.15 GPa. Pulay stress corrections were evaluated numerically based on the method introduced by Francis and Payne[23] using the total energy calculated at three different values of the kinetic energy cutoff.

III. Results and Discussion

A. Crystallographic Parameters. The various optimizations of the unit cell have been done using a cutoff energy of 1500 eV, a value that is high enough to give an accurate description of the crystallographic parameters. A number of 2k-points were used for Brillouin zone sampling, which were generated using

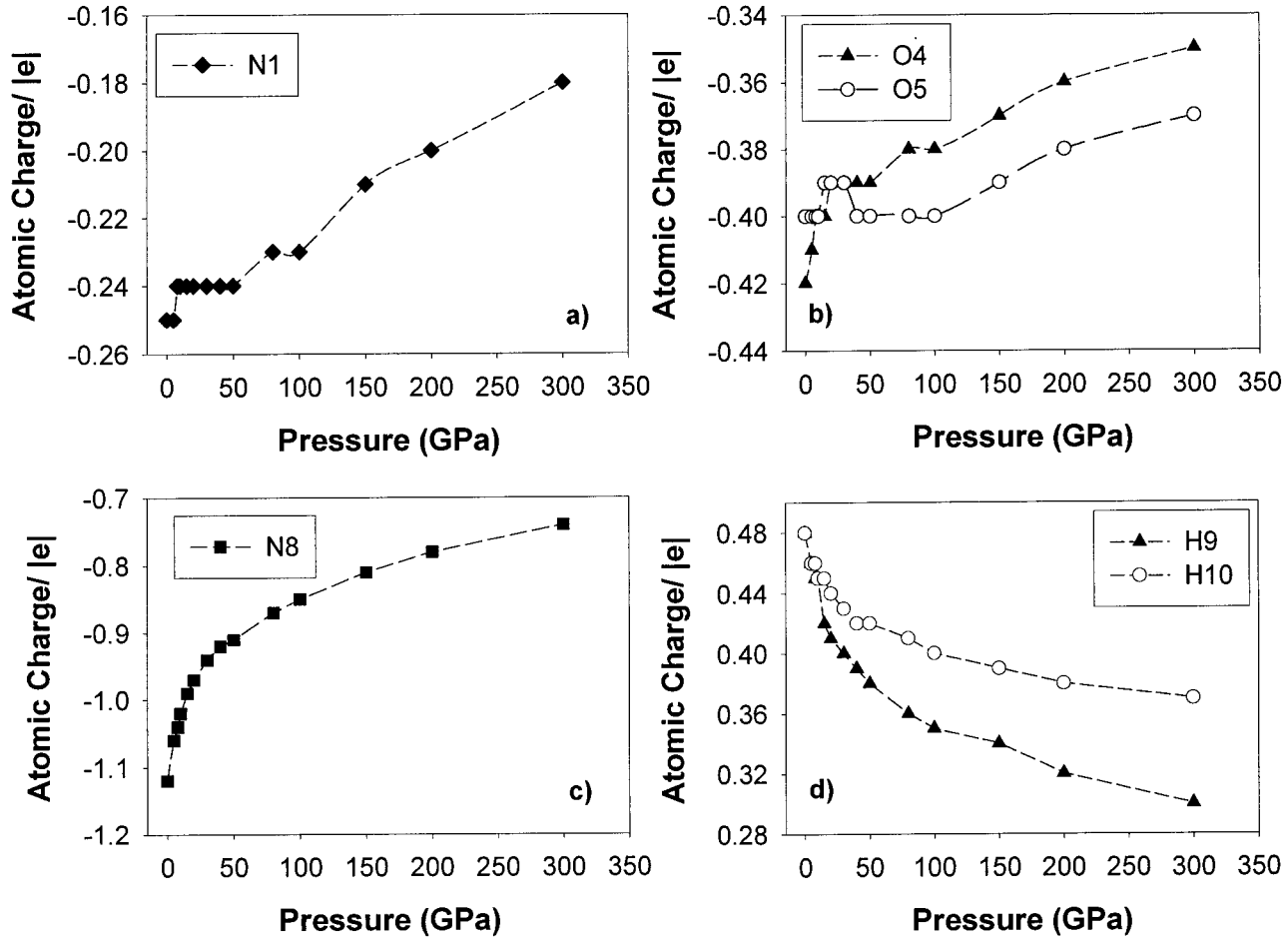

Figure 8. Variation of the Mulliken charges assigned to the atoms of NH_4^+ and DN^- as functions of pressure.

the Monkhorst-Pack scheme[20] with mesh parameters 2 × 1 × 2 along the three reciprocal lattice vectors. The optimized lattice parameters determined for the zero pressure case are $a = 7.081$ Å, $b = 12.001$ Å and $c = 5.660$ Å. These values deviate by 2.42%, 1.82%, and 0.82%, respectively, from those determined by X-ray measurements.[2] The predicted β angle of the unit cell is 101.2°, which is only 0.79% larger than the experimental value of 100.4° while the other two angles of the unit cell α and γ remain equal to the experimental value of 90.0°, consistent with space group symmetry $P2_1/c$. The discussion of specific geometrical parameters of dinitramide and ammonium ions has been done in detail in our previous study[16] and it will not be repeated here.

The compressibility of ADN has been investigated for the pressure range 0−300 GPa. Pictorial views of the conformations of the ADN unit cell for pressures of 0, 10, 40, and 150 GPa are given in Figure 1. The structures in Figure 1 show that the shape of the unit cell undergoes significant deformation with increasing pressure. The dinitramide ions deform while the ammonium ion reorients relative to the anions.

We first discuss the effects of pressure on the unit cell dimensions. The volume and unit cell angles as functions of pressure are shown in Figures 2 and 3. As can be seen in Figure 2a the largest compression of the unit cell takes place in the region of low pressures below 10 GPa, where the compressibility is anisotropic. The structure is much stiffer in the *a* and *c* directions than along the *b* axis. Fits of the data close to ambient pressure indicate a compressibility almost equal for the *a* and *c* axes of about 0.08 Å/GPa and of 0.15 Å/GPa for the *b* axis. As was pointed out by Gilardi et al.,[2] the ADN crystal contains two independent three-dimensional networks of H-bonds. The first one involves a hydrogen-bonding chain propagating along the *c* axis which is then repeated at different distances along the *b* axis. The second network, which is along the *a* axis, has an approximate helix pattern that also repeats down along the *b* axis. The H-bonds are stronger in the ac plane than in the *b* direction, causing greater compressibility along the *b* axis. These values are also consistent with our previous results for the anisotropy in the thermal expansion of ADN;[16] that is, the thermal expansion along the *b* direction is greater than in the *a* and *c* directions.

Increasing the pressure above 20 GPa leads to a decrease of about an order of magnitude in the linear compressibility along the three axes. For example, at 20 GPa the calculated compressibilities have values of 0.0080 Å/GPa, 0.015 Å/GPa, 0.0073 Å/GPa for the *a*, *b* and *c* directions, respectively. At even higher pressures the behaviors of the lattice parameters are similar as indicated by the almost parallel curves in Figure 2a for the high-pressure regime.

From the pressure dependence of the unit cell volume (see Figures 2b and 2d) we have determined the bulk modulus of ADN crystal based on a fit to the third-order Birch−Murnaghan equation of state[24]

$$p(V) = \frac{3}{2} b_0 \left[\left(\frac{V_0}{V}\right)^{7/3} - \left(\frac{V_0}{V}\right)^{5/3}\right] \left\{1 + \frac{3}{4}(b'-4)\left[\left(\frac{V_0}{V}\right)^{2/3} - 1\right]\right\} \quad (1)$$

where V_0 is the unit-cell volume at zero pressure, b_0 is the bulk modulus, and $b' = \partial b/\partial p$. When we considered only the volume

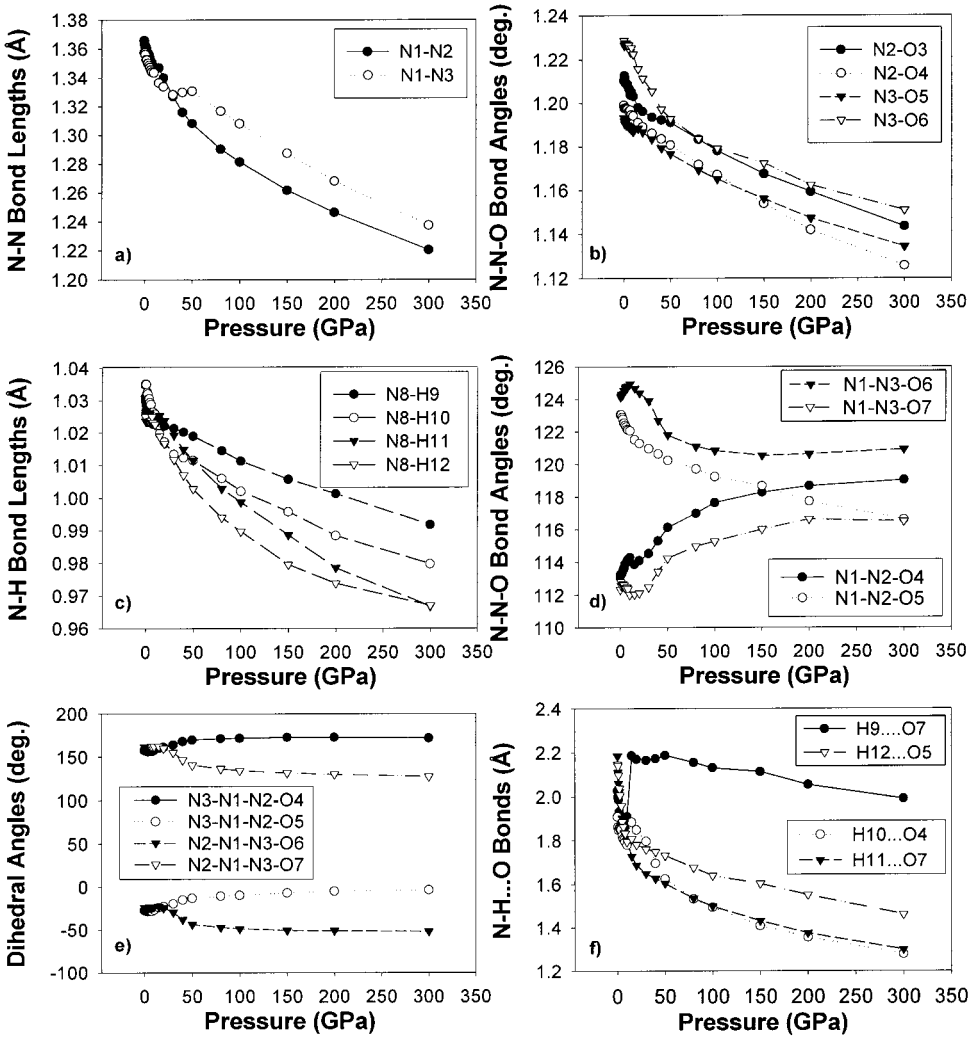

Figure 9. Selected intramolecular and intermolecular geometrical parameters of NH_4^+ and DN^- as functions of pressure.

data in the low-pressure regime below 10 GPa (see Figure 2c) the corresponding values of the fit are $V_0 = 472.55$ Å^3, $b_0 = 20.65$ GPa, and $b' = 4.03$. The calculated V_0 parameter is in good agreement with the predicted unit cell volume at ambient pressure of 471.9 Å^3. However, when the fit is done over the entire range of 0−300 GPa the parameters are $V_0 = 461.3$ Å^3, $b_0 = 22.29$ GPa, and $b' = 4.75$.

Several main regions can be identified in the behavior of the unit cell angles with pressure (see Figure 3). In the low-pressure regime between 0 and 5 GPa the unit cell angles remain practically unchanged relative to the ambient pressure values. Both the α and γ angles remain equal to 90.0°, consistent with the $P2_1/c$ symmetry. In the pressure range 5−10 GPa both angles α and β start to increase. However, over this pressure range the deviation of the α angle from 90.0° still remains very small, only reaching 90.44° at 10 GPa. The overall crystal symmetry remains monoclinic in this pressure range. Above 20 GPa the unit cell deformations become significantly larger and they increase with increasing pressure, while the crystal symmetry is changed from monoclinic to $P\bar{1}$ triclinic symmetry.

B. Electronic Properties. A first analysis of the electronic properties of ADN crystal is based on evaluation of the total density of states (DOS) and projected density of states (PDOS) on atom-centered orbitals; these are shown in Figure 4. The contributions of the individual atoms in the ammonium and dinitramide ions to the PDOS are given in Figure 4b−e. Comparisons of Figures 4a and 4b−e reveals that the individual s and p bands corresponding to different atoms can be identified clearly in the total DOS spectrum excepting the regions between (−9.5, −5) eV and (−2.7, 0) eV, where a mixing of states from the ammonium and dinitramide ions is present, consistent with the molecular character of the crystal. Comparing the results in Figure 4a with 4b and 4c shows that the top of the valence band is represented by the O(2p) and N_1(2p) levels. The next occupied band centered around −3.4 eV has contributions mainly from the N_1(2s) atom in the DN^- ions. The bottom of the conduction band or the lowest unoccupied crystalline orbitals centered at 3.1 and 4.6 eV are formed by contributions from both the O(2p) as well as the N_1(2p) and N_2(2p) atoms of the DN^- ions.

Additional insight in the effects of pressure on the electronic structure of ADN has been obtained from calculations of the band structure and density of states as functions of pressure; the results are given in Figures 5 and 6. In the case of the two lowest pressures, 0 and 10 GPa, the symmetry of the crystal is monoclinic while for the higher pressures 40 and 150 GPa the symmetry is triclinic. The band gap continuously decreases from about 3 to 2.3 eV over the range 0−150 GPa, corresponding to a variation in the unit cell volume of about 58%. Upon compression there is a significant increase of the width of different groups of bands. This effect starts at the top of the valence bands (Figure 5b shows the low-pressure regime) and extends to deeper bands at higher pressures (see Figure 5, parts c and d). Accompanying the broadening, there are shifts of the

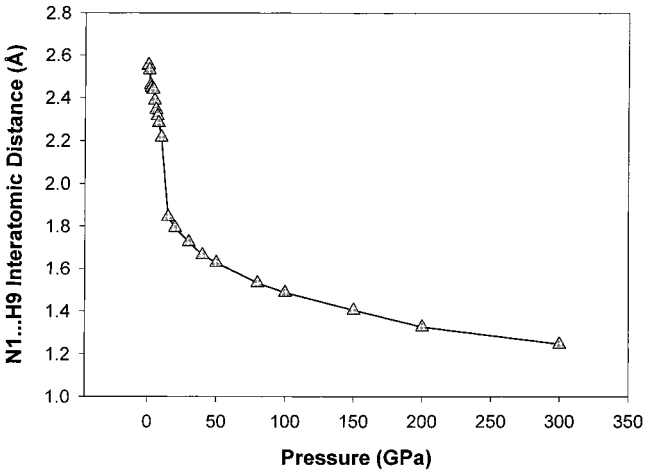

Figure 10. The variation of $N_1...H_9$ intermolecular distance as a function of pressure.

bands to lower energies with increasing pressure. These effects are due to the increase of charge overlap and delocalization among different atoms in the system.

C. Charge Variations. A pictorial illustration of the variation of the charge distribution as a function of hydrostatic compression is given in Figure 7. In Figure 7 the section through the charge density distribution is taken in a plane parallel to the aOc crystallographic plane passing through the N_8 atom of the ammonium ions. By comparing the distributions at 0 and 300 GPa we see two major effects. The first one is determined by the spread of charge around the individual ions leading to increased charge overlap. The second effect is charge transfer and redistribution among various atoms.

The charge redistribution effects can be more clearly understood by examining the Mulliken charges of the atoms, which provide a qualitative description of the bonding character. These quantities were determined using the formalism developed by Segall et al.[25] as incorporated in the CASTEP package. Selective variations of the individual atomic Mulliken charges as functions of pressure are shown in Figure 8. The largest charge variations take place for the N_1 atom of DN^- and the N_8 atom in the ammonium ion. In both these cases the charges decrease in absolute values with increasing pressure. For example, the charge variation for the N_8 atom is $-0.38e$ over the entire pressure range. However, in the case of the N_2 and N_3 atoms (not shown in Figure 8) in the dinitramide ion, the charge variations remain extremely small, below 0.01e, with increasing pressure. The absolute charges of the oxygen atoms of DN^- undergo similar decreases (less than 0.1e), but the maximum variations are smaller than for the N_8 atoms. Corresponding to these changes, the positive charges of the H atoms continuously decrease with pressure, reaching a maximum variation of 0.18e over the pressure interval 0−300 GPa. The total charge of the DN^- ion changes from about $-0.82e$ at zero pressure to $-0.58e$ at 300 GPa. This charge redistribution resulting from lattice compression indicates a decrease in the ionic character of the crystal and a concomitant increase of the covalent character.

D. Intra and Inter Ionic Geometric Parameters Modifications. Finally, we have investigated the influence of increasing pressure on intramolecular geometric parameters (see Figure 9). All intramolecular distances decrease continuously over the range 0−300 GPa; by 9.7−10.6% for N−N bonds, 5.5−6.7% for N−O bonds, and 5.3−6.9% for N−H bonds. A nonmonotonic dependence is observed for some of the N−N−O bond angles (see Figure 9d); e.g., the $N_1-N_3-O_6$ angles initially increase, over the range 0−10 GPa, but this trend reverses at higher pressures. A similar behavior but in reverse order is seen for the $N_1-N_3-O_7$ angles.

The transition between the monoclinic and triclinic phases at pressures around 10 GPa takes place with rotations of the NO_2 group relative to the $N_2-N_1-N_3$ plane. Indeed, the N−N−N−O dihedral angles (see Figure 9e) practically remain equal to their values at zero pressure up to 10 GPa where significant rotations of the NO_2 groups occur. These rotations bring the atoms $N_3-N_1-N_2-O_4$ and $N_3-N_1-N_2-O_5$ essentially into the same plane, as shown in Figure 9e; that is, these dihedral angles have values close to 180° or 0°. The other NO_2 group, i.e., $N_3-O_6-O_7$ is rotated by up to 50° relative to the $N_2-N_1-N_3$ plane.

As expected, the intermolecular N−H···O distances undergo large changes with increasing pressure; e.g., the variations in the lengths of the $N_8-H_{12}\cdots O_5$, $N_8-H_{10}\cdots O_4$, and $N_8-H_{11}\cdots O_7$ H-bonds (see Figure 9f) are 31−40%. In the high-pressure regime, some of the O···H contacts, i.e., $H_{10}\cdots O_4$ and $H_{11}\cdots O_7$, decrease so much that new covalent O−H bonds are essentially formed. These modifications are consistent with the changes in the charge distributions as well as with the decrease of the ionic character of the crystal. Another important feature apparent from Figure 9f is the nonmonotonic dependence of the $N_8-H_9\cdots O_7$ intermolecular bond on pressure. This bond decreases with increasing pressure up to 10 GPa followed by a sharp increase in the 10−20 GPa region followed by a continuous decrease above 20 GPa. The rapid increase in this bond length above 10 GPa is due to the rotation of the ammonium ion relative to the dinitramide ion. In this process the H_9 atoms reorient toward the N_1 atom of DN^-, which exercises an increasingly larger interaction with the H_9 atoms as pressure increases.

Figure 10 shows the evolution of $N_1\cdots H_9$ intermolecular bond length as a function of pressure. At about 20 GPa a new H-bond $N_8-H_9\cdots N_1$ is formed. The length of this bond continues to decrease significantly with increasing pressure such that a new covalent N−H bond is practically formed at the highest pressure studied. The strong interaction between the H_9 and N_1 atoms is also apparent in the results shown in Figure 9c, from which it is clear that for the entire pressure region above 20 GPa the N_8-H_9 bond length is larger that the other three N_8-H bonds. The attraction exercised by N_1 atom for the H_9 atoms pulls them away from the N_8 atoms.

These results show that there are several significant effects when the pressure exceeds 10 GPa. First, there are decreases in the intramolecular bond lengths. Additionally, the two NO_2 groups of DN^-, which are not coplanar with one another or with the $N_2-N_1-N_3$ plane at zero pressure, rotate with increasing pressure. In this process one of the NO_2 groups, $N_2-O_4-O_5$, ends up in the same plane with the $N_2-N_1-N_3$ atoms while the other NO_2 group is rotated from this plane by about 50°. Corresponding to these changes the nonbonded intramolecular $O_5\cdots O_6$ distance decreases by 15%, from 2.595 to 2.206 Å. Finally, the orientations of the ammonium ions relative to the dinitramide ions are maintained up to about 10 GPa, where the NH_4^+ ions reorient as indicated by the nonmonotonic change in the $N_8-H_9\cdots O_7$ bond length and the formation of the new $N_8-H_9\cdots N_1$ H-bond. The rotated position of NH_4^+ ions can also be seen in Figure 1 parts c and d.

IV. Summary and Conclusions

The results of these calculations demonstrate that a detailed description of the hydrostatic compression effects on structural and electronic properties of crystalline ADN can be obtained using plane-wave total energy calculations based on DFT theory and the pseudopotential method.

It was found that at ambient pressure the DN^- ion has inequivalent N−N and N−O bond distances and that the nitro groups are twisted from the $N_1-N_2-N_3$ plane, in agreement with experiments.[2] This is mainly due to minimization of the steric effects between the O_5 and O_6 atoms and maximization of the conjugation between the NO_2 groups and the lone pairs on the central nitrogen atom.

The results of band structure calculations and the analyses of the density of states indicate that ADN is an electrical insulator with a band gap of about 3.1 eV at ambient pressure. The structure of the occupied bands is characterized by the lack of dispersion along the Brillouin zone. The separations of the different groups of bands are as large as a few eV. The top of the valence band is given by contributions of O(2p) and N_1(2p) atoms of DN^- ion.

Under hydrostatic compression ADN maintains monoclinic symmetry up to about 10 GPa, above which a transition to a triclinic structure of $P\bar{1}$ symmetry occurs. In the low-pressure regime the compression is highly anisotropic, with compression along the *b* axis being about twice as large as along the *a* and *c* axes. In the high-pressure regime the compression becomes more isotropic due to the increase of charge overlap and changes in the bonding character toward covalent. The calculated bulk modulus at zero pressure determined from the variation of the lattice volume with pressure based on Birch−Murnaghan equation of state is $b_0 = 20.6$ GPa.

Increasing the pressure has strong effects on the electronic properties of the crystal. Mainly there are large broadenings of the electronic occupied bands with shifts toward lower energies. A monotonic drop of the band gap by about 25% from the ambient pressure value occurs over the range 0−150 GPa.

Simultaneously with these effects, there is significant charge redistribution among the atoms of the crystal with increasing pressure leading to a decrease in the ionic character of the crystal.

Finally, increasing pressure significantly influences the orientations of the NO_2 groups relative to the $N_2-N_1-N_3$ plane and causes reorientations of the ammonium ions relative to the DN^- ions. This reorientation is accompanied by a sharp decrease of three of the four N−H···O H-bonds of the ammonium ions and leads to formation of new covalent O−H and N_1−H bonds.

Acknowledgment. This work was supported by the Air Force Office of Scientific Research (Grant No. F49620-00-1-0273). We thank Dr. Richard D. Gilardi of the Naval Research Laboratory, Washington, DC, for making available to us the crystallographic parameters of the ADN crystal.

References and Notes

(1) Bottaro, J. C.; Schmidt, R. J.; Renwell, P. E.; Ross, D. S. World Intellectual Property Organization, International Application Number PCT/US91/04268, December 26, 1991.

(2) Gilardi, R.; Flippen-Anderson, J.; George, C.; Butcher, R. J. *J. Am. Chem. Soc*. **1997**, *119*, 9411, and references herein.

(3) Martin, A.; Pinkerton, A. A.; Gilardi, R. D.; Bottaro, J. C. *Acta Crystallogr*. B **1997**, *53*, 504.

(4) Russell, T. P.; Piermarini, G. J.; Miller, P. J. *J. Phys. Chem*. B **1997**, *101*, 3566.

(5) Politzer, P.; Seminario, J. M.; Concha, M. C.; Redgern, P. C. *J. Mol. Struct.* (THEOCHEM) **1993**, *287*, 235.

(6) Michels, H. H.; Montgomery, J. A., Jr. *J. Phys. Chem*. **1993**, *97*, 6602.

(7) Mebel, A. M.; Lin, M. C.; Morokuma, K.; Melius, C. F. *J. Phys. Chem*. **1995**, *99*, 6842.

(8) Rossi, M. J.; Bottaro, J. C.; McMillen, D. F. *Int. J. Chem. Kinet*. **1993**, *25*, 549.

(9) Brill, T. B.; Brush, P. J.; Patil, D. G. *Combust. Flame* **1993**, *92*, 178.

(10) Russell, T. P.; Stern, A. G.; Koppes, W. M. *Proceedings of the JANNAF Combustion Meeting*, Hampton, VA, Oct. 19, 1992**;** Vol. 23, p 5646.

(11) Vyazovkin, S.; Wight, C. A. *J. Phys. Chem. A* **1997**, *101*, 5653. Ibid. **1997**, *101*, 7217.

(12) Oxley, J. C.; Smith, J. L.; Zheng, W.; Roger, E.; Coburn, M. D. *J. Phys. Chem*. A **1997**, *101*, 5646.

(13) Fetherolf, B. L.; Litzinger, T. A. *Combust. Flame* **1998**, *114*, 515.

(14) Tompa, A. S. *Thermochim. Acta* **2000**, *357*, 177.

(15) Russell, T. P.; Piermarini, G. J.; Block, S.; Miller, P. J. *J. Phys. Chem*. **1996**, *100*, 3248.

(16) Sorescu, D. C.; Thompson D. L. *J. Phys. Chem*. B **1999**, *103*, 6774.

(17) Russell, T. P.; Tran, Y.; Gotezmer, C.; Bedford, C. D. CPIA *Publication Proceedings of the JANNAF Propulsion Meeting*, Indianapolis, IN, Feb. 1992.

(18) Milman, V.; Winkler, B.; White, J. A.; Pickard, C. J.; Payne, M. C.; Akhmatskaya, E. V.; Nobes, R. H. *Int. J. Quantum Chem*. **2000**, *77*, 895.

(19) White, J. A.; Bird, D. M. *Phys. Rev*. **1994**, *B50*, 4954.

(20) Monkhorst, H. J.; Pack, J. D. *Phys. Rev*. **1976**, *B13*, 5188.

(21) Kleinman, L.; Bylander, D. M. *Phys. Rev. Lett*. **1980**, *45*, 566.

(22) Lin, J. S.; Qteish, A.; Payne, M. C.; Heine, V. *Phys. Rev*. **1993**, *B47*, 4174.

(23) Francis, G. P.; Payne, M. C. *J. Phys. Condens. Matter* **1990**, *2*, 4395.

(24) Poirier, J. P. *Introduction to the Physics of the Earth's Interior*; Cambridge University Press: Cambridge, U.K., 1991.

(25) Segall, M. D.; Pickard, C. J.; Shah, R.; Payne, M. C. *Phys. Rev*. **1996**, *B54*, 16317.